University of Bath

Alternative formats
If you require this document in an alternative format, please contact:
openaccess@bath.ac.uk

1 **Orange juice ultrafiltration: Characterisation of deposit layers and membrane surfaces**
2 **after fouling and cleaning**
3

4 Nurul Hainiza Abd-Razak[1,2], Y.M. John Chew[1], Michael R. Bird[1*]

5 [1]Centre of Advanced Separations Engineering, Department of Chemical Engineering, University of
6 Bath, Bath BA2 7AY, UK

7 [2]Rubber Research Institute of Malaysia, Malaysian Rubber Board, PO Box 10150, 50908 Kuala Lumpur,
8 Malaysia

9 *Corresponding author. Email address: M.R.Bird@bath.ac.uk

10

Abstract

12 The influence of feed condition and membrane cleaning during the ultrafiltration (UF) of orange juice
13 for phytosterol separation was investigated. UF was performed using regenerated cellulose acetate
14 (RCA) membranes at different molecular weight cut-off (MWCO) values with a 336 cm^2 membrane
15 area and a range of temperatures (10 – 40°C) and different feed volumes (3 - 9 L). Fluid Dynamic
16 Gauging (FDG) was applied to assess the fouling and cleaning behaviours of RCA membranes fouled
17 by orange juice and cleaned using *P3-Ultrasil 11* over two complete cycles. During the FDG testing,
18 fouling layers were removed by fluid shear stress caused by suction flow. The cleanability was
19 characterised by using *ImageJ* software analysis. A Liebermann-Buchard-based method was used to
20 quantify the phytosterol content. The results show that RCA 10 kDa filters exhibited the best
21 separation of phytosterols from protein in orange juice at 20 °C using 3 L feed with a selectivity factor
22 of 17. Membranes that were fouled after two cycles showed higher surface coverage compared to
23 one fouling cycle. The surface coverage decreased with increasing fluid shear stress from 0 to 3.9 Pa.
24 FDG achieved 80 to 95% removal at 3.9 Pa for all RCA membranes. Chemical cleaning using *P3-Ultrasil
25 11* altered both the membrane surface hydrophobicity and roughness. These results show that the
26 fouling layer on RCA membranes can be removed by fluid shear stress without affecting the membrane
27 surface modification caused by chemical cleaning.

28

29 **Keywords:** Ultrafiltration; Orange juice; Fouling; Fluid dynamic gauging; Shear Stress

30

31

1 Introduction

In the recent decades, ultrafiltration (UF) has grown to be an important process for industrial uses such as food processing [1] and recovery of bioactive compounds [2] and wastewater treatment [3]. Membrane processes are of great interest in reducing the number of unit operations required, recycling process water and reducing operating costs [4]. However, the separation efficiency of membrane filtration can be limited by membrane fouling. Fouling refers to the accumulation of unwanted material on the membrane surface and/ or inside the membrane pores during the filtration. Membrane fouling resulted in low permeate flux, reduced productivity, increased feed pressure, altered membrane properties and shortened membrane life [5]. Fouling depends upon membrane surface chemistry, hydrophobicity, surface roughness and surface charge [6, 7]. Fouling is also reliant on operational conditions such as flow rate, transmembrane pressure and the concentration of feed components [8]. Temperature is a key factor in membrane filtration for juice processing such as UF to separate anthocyanins, naritunin and hesperidin from orange juice [9] and to recover anthocyanin from black currant juice [10]. Therefore, the influence of temperature and feed concentration are essential to study in order to maintain the separation performance.

Cleaning techniques such as chemical cleaning, mechanical cleaning, electric and hydraulic cleaning have been used to regenerate membranes. The cleaning method selected depends upon the arrangement of the membrane module, the type of the membrane, the nature of the fouling layer and the degree of fouling present [11]. Cleaning-in-place is applied by using cleaning agents such as acids, alkalis, oxidants, surfactants, enzymes or a combination thereof. The cleaning agent typically restores the membrane by dissolving or chemically changing the fouling layer [12]. The chemical agents can easily modify the membrane properties, thereby altering the filtration selectivity, reduce the membrane lifespan and increase operational cost [13]. Mechanical cleaning has been applied to tubular membrane modules using sponge balls [8], but this cleaning method was not able to remove organic foulants formed inside the membrane pores. The use of mechanical cleaning in membrane bioreactors by using scouring agents was developed as a novel approach to controlling membrane fouling [14]. The efficiency of mechanical cleaning is highly dependent on the type of foulant present. Small particles such as proteins may be difficult to remove from the membrane surface using scouring agents.

Fluid dynamic gauging (FDG) is a method for determining the thickness of soft fouling layers deposited on both non-porous surfaces [15] and porous substrates [16]. Fluid dynamic gauging (FDG) has been employed to estimate the thickness of fouling layers of molasses solution deposited on microfiltration membranes [17] and to measure the strength of a softwood Kraft lignin on RCA membrane during the cross-flow microfiltration [18]. Interestingly, FDG was also applied to monitor the removal of cake layers in membrane cleaning through thickness measurement with controlled application of fluid shear to the cake layer's surface [19]. Mechanical cleaning using FDG technique is reported in this paper, and is compared to the chemical cleaning that has been used in our previous research [20]. Membranes subjected to chemical cleaning were found to display modified surface hydrophobicity, roughness [20] and charge [21].

The aims of this study are to (i) assess the effect of operating conditions such as temperature and feed volume upon the recovery of phytosterols from orange juice and to (ii) evaluate the cleanability of the membranes by chemical and/ or mechanical/ hydraulic cleaning. The novelty of this work is in the application of FDG to study cleaning of fruit juice foulants formed on UF membranes. The purpose of using FDG is both in the quantification of the shear stress required to remove the fouling layers, and in the determination of the need for chemical cleaning to achieve an effective restoration of filtration performance.

2 Materials and Methods

2.1 Orange juice, solvents and standards

Processed orange juice (not from concentrate) was obtained from a UK processor where the juice was prepared by using extraction and centrifugation (*Cobell*, UK). Solvents and reagents used such as chloroform, methanol, acetic anhydride and sulphuric acid were obtained from *Merck*, UK. Characterisation standards used are stigmasterol from *Sigma Aldrich*, UK and protein assay kit from *Bio-Rad*, UK. The chemical cleaning after fouling was carried out using 0.5% *P3-Ultrasil 11* (*Henkel Ecolab*, USA) [22].

2.2 Ultrafiltration experiment

UF experiments were carried out using regenerated cellulose acetate (RCA) flat-sheet membranes from *Alfa Laval* (Denmark) that installed in a cross flow filtration apparatus *LabStak M10*, developed by *Alfa Laval* (previously *DSS*) (Denmark) with a 336 cm^2 membrane area. The UF cycle comprises of membrane conditioning, pure water flux (PWF), ultrafiltration, rinsing and cleaning steps were described previously [23]. The orange juice was filtered in recycling mode. The permeate was collected in a beaker and the retentate was recycled back into the feed tank.

There are two parts of experiments in this study. All UF experiments were done in triplicate. Investigation into the effect of feed conditions (temperature and feed volume) during the UF of orange juice was carried out using a 10 kDa membrane (Code RC70PP,*Alfa Laval*, Denmark). The operating temperature range for RCA membranes suggested by Alfa Laval is 5 to 60 °C. To study the effect of different feed conditions, the temperature of the feedstock during the UF using 10 kDa RCA membrane was adjusted from 10 to 40 °C and the orange juice feed volume used was 3L, 6L and 9L.

In the second part of this study, RCA membranes at three different MWCO values (10 kDa, 30 kDa and 100 kDa) were used for the investigation of membrane cleaning. The membrane characteristics have been summarised previously in Abd Razak et al., (2020). In order to study the influence of different membrane cleaning, the UF using RCA membranes were performed at 20°C using 3L orange juice. The membranes were cleaned by using chemical cleaning agent *P3-Ultrasil 11* at 60 °C for 10 minutes with a TMP of 1.0 bar. Mechanical cleaning was performed using fluid dynamic gauging (FDG) at 20 °C. These experiments are summarised in Figure 1.

2.3 Fluid dynamic gauging (FDG)

Fluid dynamic gauging (FDG) has been shown to be a non-contact technique to assess the thickness and strength of surface deposits [18, 19, 24]. Figure 2 and Figure 3 illustrate the apparatus used in this FDG study. This method works by forcing a constant flow of fluid into the FDG nozzle. The suction flow into the gauge creates fluid shear stress (τ) on the fouling layers, to remove the foulant from the membrane surface. The fluid shear stress can be estimated by using Equation (1):

$$\tau = \frac{3\mu m}{\rho \pi h^2 r} \tag{1}$$

where μ is the fluid dynamic viscosity, m is the gauging mass flow rate, ρ is the fluid density, h is the gap between the fouling and the gauge, and r is the inner radius of the FDG nozzle. Peck et. al (2015) who studied the removal of biofilms deposit suggested that the shear stress forced by the gauging flow is associated to the mean pipe flow velocity (μ_{min}) as shown in Equation (2):

$$\mu_{min} = \sqrt{\frac{2\,\tau_{wall}}{\rho\,C_f}} \qquad\qquad (2)$$

Where τ_{wall} is the wall shear stress, C_f is the friction factor, and ρ is the fluid density. The friction factor (C_f) is equal to 0.005 for turbulent flow regimes.

The shear stress on the surface due to gauging flow relies on the dimensionless value of h/d_t and flow conditions [25]. Figure 2(a) shows the schematic of a FDG nozzle. Figure 2(b) shows an example of a fouled RCA membrane. The dashed line shows a dimension and footprint of the FDG nozzle inner diameter, d_t = 5 mm and nozzle outer diameter = 10 mm. The FDG nozzle was installed in a custom-made test rig as described in Figure 3. RO water was used as the process fluid for FDG tests that is drawn through a nozzle at a constant flow rate of 25 ml min^{-1}. The suction flow was controlled by a digital mass flow meter (*mini CORI-FLOW*, Bronkhorst, UK). A fouled membrane was cut and mounted on the stainless-steel plate placed under the FDG nozzle. The gauging nozzle was placed in the middle of the membrane sample that installed on the stage as shown in Figure 3. Measurements were performed for known values of h/d_t at difference nozzle clearance heights to impose difference in shear stress. All h/d_t measurements were done in triplicate. A micrometer (*Mitutoyo*, Japan) was used to adjust the vertical movements of the gauge and to measure the clearance height from the membrane. The system was controlled and monitored by using a *LabView* visual interface. All images of fouled and cleaned membranes were captured using the *Samsung A3* camera. The removal of fouling layers on the membrane surfaces was analysed using *ImageJ* analysis by measuring the percentage area of the membrane that covered with the foulants, with a known scale bar to convert the actual pixels on the images.

2.4   Fouling and cleaning experiment

RCA membranes at different   MWCO values were fouled with orange juice over two fouling-cleaning cycles and cleaned using two different cleaning methods. Chemical cleaning was applied using 0.5% *P3-Ultrasil 11*, as mentioned in Section 2.1. Mechanical cleaning was carried out using fluid dynamic gauging (FDG) as described in Section 2.4. The fouling and cleaning cycles were performed as summarised and labelled below:

i.   **Fouled 1 (F1)** – to understand the fouling characteristics of orange juice.
ii.   **Fouled 1 (F1) → Chemical cleaning (CC)** – to investigate the effect of chemical cleaning on surface properties of membrane.
iii.   **Fouled 1 (F1) → Fluid dynamic gauging (FDG)** – to investigate the effect of mechanical cleaning imposed by FDG on surface properties of membrane.
iv.   **Fouled 1 (F1) → Chemical cleaning (CC) → Fouled 2 (F2)** – to investigate the effect of chemical cleaning on subsequent fouling behaviour.

v. **Fouled 1 (F1) → Chemical cleaning (CC) → Fouled 2 (F2) → Fluid dynamic gauging (FDG)** – to investigate the effect of chemical cleaning on subsequent fouling removal.

2.5 Membrane performance

The volumetric flow rate of the fluid through the membrane is known as the permeate flux [8]. It can be calculated according to Equation (3):

$$J = \frac{\Delta P}{\mu R_{tot}}$$ (3)

where J is the flux through the membrane (L m^{-2} h^{-1}), ΔP (Pa) is the transmembrane pressure (*TMP*), μ is the dynamic viscosity (kg m^{-1} s^{-1}) and R_{tot} is the total resistance (m^{-1}). The resistance in series is depicted in Equation (4) [26]:

$$J = \frac{\Delta P}{\mu\,(R_m + R_f + R_{cp})}$$ (4)

where R_m is the resistance of membrane, R_f is the resistance of total fouling and R_{cp} is the resistance due to concentration polarisation. The rejection ratio, R, was calculated by using Equation (5):

$$R = \left(1 - \frac{C_p}{C_r}\right)$$ (5)

where C_p is the concentration of solute in the permeate and C_r is the concentration of solute in the retentate [8]. The separation factor, $\alpha_{A/B}$, was calculated using Equation (6):

$$\alpha_{A/B} = \frac{y_A / y_B}{x_A / x_B}$$ (6)

where y_A and y_B are concentrations of phytosterols and proteins in the permeate, and x_A and x_B are concentrations of phytosterols and proteins in the feed.

2.6 Quantitative determination of compounds

2.6.1 Total phytosterols analysis

Total phytosterols content was determined spectrophotometrically by using Liebermann-Buchard (LB) based method [27, 28]. The absorbance was measured at 420 nm using an Ultraviolet-visible (UV-Vis) Spectrophotometer (*Cary 100, Agilent*, USA). The analysis was performed as described previously [23]. All measurements were done in triplicate and the results were averaged.

2.6.2 Protein analysis

The Bradford method was used to quantify the protein concentration [29, 30]. The protein concentration was measured at absorbance 595 nm using UV-Vis Spectrophotometer (*Cary 100, Agilent*, USA). The assay was carried out as described previously [23]. All measurements were performed in triplicate.

2.7 Membrane surface analysis techniques

The hydrophobicity of the membrane surface before and after fouling and cleaning was determined by measuring the contact angle via sessile drop method using *DataPhysics Optical Contact Angle System OCA 25* (Filderstadt, Germany). The surface roughness of fouled and cleaned membranes was determined using atomic force microscopy (AFM). Scanning electron microscope (SEM) images of membranes surfaces were taken with a *JEOL SEM* model *JSM 6480LV* (Japan). Contact angle measurements, surface roughness measurements and SEM analysis were conducted as described previously by Abd-Razak et al. [20].

3 Results and Discussion

3.1 Effect of feed conditions

3.1.1 Effect of temperature

During blackcurrant juice processing, the permeate flux in a UF unit operated under a total recycle mode increased by 60 % as the feed temperature rose from 25 °C to 45 °C [10]. Based on the recommended operating temperature of RCA membranes by Alfa Laval, which is in the range of 5 °C to 60 °C, the temperature of the permeate fluxes were investigated from 10 °C to 40 °C. The changes of membrane permeate flux and total fouling resistances (R_f) with operating time at different temperature are presented in Figure 4. The highest initial flux at 46 L m^{-2} h^{-1} was achieved at a temperature value of 40 °C. The initial permeate fluxes at 10 °C and 20 °C were 25 L m^{-2} h^{-1} and 29 L m^{-2} h^{-1}, respectively. This result is in agreement with the studies conducted by Pap et al. (2012) and Qaid et al., (2017) which may be due to a decrease in the solute viscosity and higher solute permeability at higher temperature. The initial flux declined gradually in the first 10 min for all three conditions. This suggests that some particles were blocking the membrane pores and larger particles were accumulating on the membrane surface which led to a reduction in filtration area. The filtration was run until 60 minutes and the permeate flux approached a pseudo steady state value after 10 min. The highest steady state permeate flux of RCA membrane was achieved at 40 °C with flux value 25 L m^{-2} h^{-1} demonstrating a flux decline of 46 %. The lowest steady state permeate flux of was achieved at 10 °C with flux value 17 L m^{-2} h^{-1} showing a flux decline of 32 %. The percentage decrease in the permeate flux as temperature increases can be explained by the effect of membrane fouling [9]. The

authors report that during the UF of blood orange juice the fouling mechanism changed to a complete pore blocking from a partial blocking as temperature increased. This means that even though 40 °C gave a higher overall flux, the extent of the decrease is more severe due to fouling.

The total fouling resistances (R_f) against filtration time for RCA membranes tested at different temperature were calculated from flux data by rearrangement of Equation (4). The graph was plotted with membrane resistance, R_m = 3 x 10^{12} m^{-1} as shown in Abd Razak et al., (2020). In this work, the concentration polarisation resistance (R_{cp}) is negligible. A concentration polarisation diagnostic test was performed in which the feed pump was turned off and then turned back on 5 minutes later. Because no change in flow was observed, it was concluded that concentration polarisation is not an important fouling-related resistance in this system. The resistance graph shows that there was a difference in fouling resistance at 40 °C. UF at 40 °C gave higher fouling resistance compared to UF at 10 °C and 20 °C. This may suggest that orange juice at higher temperature with lower viscosity produced high fouling resistance that led to membrane fouling. Black currant juice filtration at low temperature was suggested by Pap et al. (2012) to avoid precipitation of protein particles and to reduce membrane fouling. This result suggests that the operating temperature at 40 °C is not optimal for orange juice filtration.

Figure 5 shows the rejection of key compounds i.e. total phytosterols and proteins by RCA 10 kDa membranes at three different temperatures. The optimal separation would have a low rejection of phytosterols and a strong rejection of proteins. Previously, Abd Razak et al. (2020) reported that UF at 20 °C with RCA 10 kDa membrane exhibited good separation efficiency with 32 ± 4 % rejection of phytosterols and 96 ± 1 % rejection of protein. Figure 5 shows that UF at lower temperature (10 °C) using RCA 10 kDa membrane exhibited different separation efficiency with 56 ± 1 % rejection of phytosterols and 95 ± 2 % rejection of protein. The results also show that more phytosterols were collected in the permeate at higher temperatures. Therefore, an attempt has been made to run the filtration at higher temperature which was at 40 °C. As expected, lower rejection of phytosterols (35 ± 5 %) was achieved during the UF at 40 °C using RCA 10 kDa membrane. In general, proteins were highly rejected by RCA 10 kDa membrane at 10 °C and 20 °C. However, only 72 ± 2 % rejection of proteins was observed at 40 °C. Soy bean processing at high temperature (40 – 50 °C) changed the conformation of the protein structure that leads to protein precipitation [31]. Aghajanzadeh et al., (2017) studied the effect of thermal processing on proteins stability in orange juice. Temperature above 40 °C caused denaturation of proteins called pectin methylesterase (PME) in orange juice. The composition of the protein changed when hydrogen bonds were broken and the tertiary protein structure unfolded at 40 °C [32]. Therefore, it is possible that more proteins have been passed through the RCA 10 kDa membrane and collected in the permeate at 40 °C.

The mass balance for the total phytosterols and proteins following UF using 10 kDa membranes at 10 °C, 20 °C and 40 °C is presented in Table 1. In order to study the effect of temperatures, the initial feed volume of orange juice was 3 L with 830 ± 70 mg total phytosterols present in the feed solution. The yields of total phytosterols in the permeate for filtrations at 10 °C, 20 °C and 40 °C were 78 mg, 135 mg and 190 mg respectively. The mass concentration ratio of phytosterol to protein was increased from feed to permeate streams at all conditions (Table 1). The quality of separation is expressed by the separation factor of the membrane which was calculated from the mass concentration ratio. The lowest separation factor which was 2.0 can be seen in Table 1 (c) for the UF at 40 °C. This result is consistent with the rejection data (Figure 5) that showed more proteins were collected in the permeate probably due to the changes in membrane pore size at high temperature [33]. UF using RCA 10 kDa membrane at 20 °C gave the highest separation factor which was 17.3. It is noted that the mass concentration ratio of phytosterol to protein increased from 0.3 in the feed to 5.2 in the permeate (Table 1 (b)). The loss of phytosterols and proteins at all three conditions were presumably due to the fouling effect during the filtration [29]. It is suggested that the fouling layer trapped the phytosterols, preventing them from passing through the membrane. This finding revealed that proteins can be separated from the phytosterols by UF at 20 °C.

3.1.2 Effect of feed volume

In this study, to address the loss of phytosterols to the foulant layer, the total amount of feed filtered was increased while the membrane area remained constant. It is hypothesised that filtration with larger feed volume can be used to increase the total amount of sterol present in the system. The UF was carried out at 20 °C based on the results from previous experiment. In Figure 6 there is a clear trend of decreasing permeate flux with operating time at three different feed volumes. Figure 6 shows that the initial permeate fluxes for all membranes were almost similar (26 ± 1 L m^{-2} h^{-1}). The initial permeate fluxes using 3 L, 6 L and 9 L orange juices decreased as the filtration time increased until it reached steady-state values of 23 L m^{-2} h^{-1}, 19 L m^{-2} h^{-1} and 18 L m^{-2} h^{-1} at approximately 12 minutes. The initial fluxes declined gradually within the first 10 min for all three conditions. It is likely that the membranes were fouled which led to a reduction of filtration area. After the 60 min filtration, UF using 6 L and 9 L orange juices showed lower permeate flux compared to 3 L feed volume. This is likely due to the higher concentration of proteins in high volume of feed solution which caused the membrane fouling. The loss of proteins in feed solution were possibly due to the interaction of the solute with the membrane and the adsorption of the solute on the membrane surface or within the pores [29].

Table 2 presents a mass balance and separation factor for total phytosterols and proteins by UF with 10 kDa RCA membranes using three different feed volumes; 3 L, 6 L and 9L orange juices. In this experiment, the initial total phytosterols present in feed solution were varied from 810 mg in 3 L orange juice to 2430 mg in 9 L orange juice. Meanwhile the initial proteins in feed solution were of 2910 mg and 8640 mg for 3 L and 9 L orange juice. This is in agreement with the hypothesis that larger feed volume offered larger amount of phytosterol in the system. The mass concentration ratio of sterol to protein was increased from feed to permeate streams at all conditions (Table 2). The mass concentration ratio of sterol to protein increased from 0.3 in the feed to 5.2 in the permeate for the UF using 3 L orange juice. 9 L orange juice produced mass concentration ratio of sterol to protein from 0.3 in the feed to 4.6 in the permeate. The separation factor (Equation 4) for the UF using 3 L, 6 L and 9L orange juices were 17.3, 13.0 and 15.3 respectively. It can be noted that increasing feed volume could not improve the separation efficiency in this system.

Table 2 also shows that there was insignificant difference in volume of permeate after 60 min filtration for all three conditions. UF using 3 L orange juice produced 850 ml permeate. Interestingly, 800 ml permeate was collected from the filtration using larger feed volume which was 6 L and 9 L orange juice. This means that less total phytosterols can be collected in the permeate. The lower separation factor seen in Table 2 for 6 L and 9 L orange juice are possibly related to a higher protein loss into the cake layer. The 22 % loss of proteins in the system at 6 L feed volume and 23 % loss for 9 L feed volume were most likely affected by fouling during filtration [29]. It is possible that the phytosterols were trapped by the fouling layer, which is made up of proteins, and did not pass through the membrane. This study discovered that the best separation of phytosterols from proteins in orange juice by UF using RCA membranes at cross flow velocity (CFV) of 1.5 m s^{-1} can be achieved by using 3 L feed volume. In the future, this process can be improved by increasing the CFV to increase the permeate flux in order to achieve higher permeate volume.

3.2 Membrane fouling and cleaning

3.2.1 Fluid dynamic gauging (FDG)

The cleaning of regenerated cellulose membranes using FDG was carried out in order to compare its efficacy with that of the chemical cleaning method. The purpose of using FDG is to measure the shear stress required to eliminate the fouling layers and to determine if chemical cleaning is sufficient to achieve effective cleaning. FDG has previously been shown to be a useful tool for determining the thickness and strength of the fouling layer during membrane filtration [17, 18]. However, the fouling layers obtained in this work were too thin and the fouling layer thickness could not be determined reliably. Therefore, the surface coverage of the membranes was analysed using *ImageJ* analysis to characterise removal of fouling deposits by using FDG.

Figure 7 (a) shows the images of FDG cleaning for RCA 10 kDa after first fouling-cleaning cycle (**(F1)** → **(FDG)**). The images of FDG cleaning for RCA 10 kDa after second fouling-cleaning cycle (**(F1)** → **(CC)** → **(F2)** → **(FDG)**) are presented in the Supporting Information. For RCA 10 kDa (**(F1)** → **(FDG)**), the surface coverage decreased from 84 ± 2 % to 4 ± 2 % at shear stress from 0 Pa to 3.9 Pa. The same trend was observed in RCA 10 kDa (**(F1)** → **(CC)** → **(F2)** → **(FDG)**) with surface coverage decreased from 87 ± 4 % to 8 ± 2 % at shear stress from 0 Pa to 3.9 Pa. These results indicate that RCA 10 kDa membranes which were fouled twice gave a slightly higher surface coverage compared to one-time fouling. Previous work in our laboratory by Abd Razak et. al (2020) postulated that the RCA 10 kDa membrane was fouled with a cake of proteins, which the 10 kDa membrane strongly rejected. Hydrophilic membranes like RCA 10 kDa were found to have a greater extent of reversible than irreversible fouling.

The FDG cleaning for RCA 30 kDa (**(F1)** → **(CC)** → **(F2)** → **(FDG)**) is shown in Figure 7 (b). Figure 10 in the Supporting Information presents the images of FDG cleaning for RCA 100 kDa membrane. At shear stresses from 0 Pa to 3.9 Pa, the surface coverage of RCA 30 kDa (**(F1)** → **(FDG)**) and RCA 30 kDa (**(F1)** → **(CC)** → **(F2)** → **(FDG)**) were 88 ± 3 % to 9 ± 3 % and 94 ± 2 % to 13 ± 2 % respectively. These results suggest that the surface coverage after two-times fouling was higher than that for one-time fouling. Abd Razak et. al (2020) reported that for both RCA 30 kDa and RCA 100 kDa membranes, intermediate pore blocking was the most common fouling mechanism. Larger pore membranes may have allowed protein-based foulants to penetrate the structure more deeply. Thus, a higher shear stress is needed to achieve a greater removal of fouling from these two membranes. In general, Figure 7 shows that the surface coverage decreased with increasing shear stress from 0 to 3.9 Pa for all membranes. It is likely that the RCA 10 kDa membrane was cleaned more easily using FDG than either the RCA 30 kDa or the RCA 100 kDa membranes, as the RCA 10 kDa membrane showed the lowest surface coverage. This result indicates that mechanical cleaning using fluid shear stress did not alter the subsequent fouling behaviour of the membrane.

Figure 8 shows the surface coverage of RCA membranes after FDG cleaning at four different shear stress values, from 0.28 to 3.9 Pa. Open symbols in Figure 8 represent the first fouling-cleaning cycle (**(F1)** → **(FDG)**) and close symbols represent second fouling-cleaning cycle (**(F1)** → **(CC)** → **(F2)** → **(FDG)**). It is clear that the surface coverage for all membranes decreased with increasing shear stress from 0.28 to 3.9 Pa (Figure 8). Membranes that were fouled twice gave higher surface coverage compared to one-time fouling for all samples examined. This is consistent with findings from the *ImageJ* analysis. RCA 30 kDa membranes showed the highest surface coverage at shear stress values of 0.62 and 1.73 Pa. RCA 100 kDa showed the highest surface coverage at shear stress values of 0.28 and 3.90 Pa. Figure 8 also shows that mechanical cleaning using FDG achieved 82 - 95% removal at 3.9 Pa. It was clear that RCA 10 kDa was the membrane most easily cleaned using FDG, as it showed the lowest surface coverage for shear stress values of 0.28 to 3.9 Pa. It can be concluded that fouling removal on RCA 10 kDa was achieved by applying lower shear stress. Meanwhile, higher shear stress was needed to remove foulants on other membranes. For comparison in Fig 7, the same shear stress at 0.62 Pa produced 65 % surface removal for RCA 10 kDa and 38 % surface removal of RCA 30 kDa membrane. The fluid velocity can be calculated from the shear stress values using Equation (2). For a turbulent flow at 3.9 Pa, the fluid velocity (water was used in this case) was 1.3 m s^{-1}. This result shows that the FDG can be used to optimise the cross-flow velocity (CFV) used during PWF and rinsing in the

cleaning process. Currently, PWF and rinsing were carried out using reverse osmosis water at CFV of 1.0 m s^{-1}. This finding indicates that a higher CFV is needed to remove the majority of reversible fouling during PWF and rinsing.

3.2.2   Membrane hydrophobicity

To investigate the effect of fouling and cleaning on the membrane properties, contact angle measurements were taken to determine the surface hydrophobicity of the RCA membrane. As the water drop contact angles measured were much less than 90° (Table 3), all of the membranes studied were found to be extremely hydrophilic. The contact angles of conditioned RCA 10, RCA 30 and RCA 100 membranes were 11 ± 2°, 13 ± 2° and 18 ± 2°, respectively. The RCA membrane hydrophobicity results recorded in this study were in good agreement to those mentioned in the literature [34-36]. Table 3 shows that the hydrophobicity of conditioned and cleaned RCA membranes changed with MWCO, with RCA100 > RCA30 > RCA10. All fouled membranes had a contact angle of 10 ± 2° after first fouling cycle. After fouling, the membranes became more hydrophilic and the hydrophobicity increased after cleaning (Table 3). The contact angle measurements for membranes after FDG cleaning (labelled as **F1→FDG**) were returned back to the pristine condition (conditioned membrane). In contrast, after first cleaning using chemical cleaning (labelled as **F1→CC**), the contact angle was lower than the conditioned membrane. For membranes which were fouled twice, first cleaned using chemical cleaning and second cleaned using FDG (labelled as **F1→CC→F2→FDG**), the contact angles were returned close to cleaned membranes after first cycle of chemical cleaning. It is postulated that chemical cleaning changed the membrane hydrophobicity because of the surfactant P3-Ultrasil 11 adsorption on the membrane surface [37]. This may suggest that mechanical cleaning using FDG is efficient in cleaning the membrane without modifying the membrane hydrophobicity.

3.2.3   Membrane surface roughness

The surface roughness of membranes before and after fouling and cleaning was investigated using atomic force microscopy (AFM). Table 4 shows that the roughness of RCA membranes varied with MWCO, RCA30 > RCA100 > RCA10. The surface roughness values of conditioned RCA 10, RCA 30 and RCA 100 membranes were 3 ± 1°, 17 ± 1° and 10 ± 2° respectively. Evans et al., (2008) also reported similar roughness value for the conditioned RCA 10 membranes. After the first FDG cleaning, Membrane surface roughnesses were restored to their original values (labelled as **F1→FDG**). However, after first treatment using chemical cleaning (labelled as **F1→CC**), surface roughness values decreased, but did not return to their original levels. This indicates that the surfaces have not been restored to their original state after chemical cleaning due to the membrane surface modification. Membranes labelled **F1→CC→F2→FDG** which were fouled twice and cleaned twice (first using chemical and second using FDG) showed surface roughness close to those seen for membranes treated by chemical cleaning alone (**F1→CC**). Thus, from this analysis, it was clear that FDG cleaning did not change the membrane surface roughness. It is therefore effective in cleaning the membrane rather than the chemical cleaning upon the surface condition of the membrane.

3.2.4   Visualisation of membrane after fouling and cleaning by SEM

The morphology of the membranes was monitored using a scanning electron microscope (SEM) under various conditions; after fouling and cleaning. Images of the surface of the RCA membranes that were

examined are shown in Figure 9. Deposition is clearly seen on the fouled membrane surfaces as shown in Figure 9 (a), (e) and (i). SEM images show that all membranes could be cleaned using chemicals and FDG after the first fouling. After the second fouling, cleaning was not as effective. This is in agreement with the surface coverage data using *ImageJ* analysis which shows the membranes that were fouled twice (labelled as (4)) gave higher surface coverage values compared to one-time fouling (labelled as (3)) for all membranes. After cleaning, the membrane surfaces changed to a smoother surface from a rough surface of fouled membranes. Cleaned membrane surfaces in Figure 9 (c, g, k) demonstrate that the FDG cleaning regime applied is effective in removing the foulants.

4   Conclusions

The optimal operating conditions for membrane separation of phytosterols from orange juice have been studied. Permeates generated using RCA 10 kDa membranes were relatively high in phytosterols, and low in protein. RCA 10 kDa membranes displayed an acceptable flux, and an effective separation of sterol from orange juice. From the conditions investigated, the most effective separation of phytosterols from protein in orange juice (with a selectivity factor of 17), was seen at a temperature of 20 °C using a 3 L feed volume. However, fouling adversely affected the performance of the membrane. Membrane cleaning is therefore needed after each filtration operation, to extend the membrane's lifetime and to preserve its efficiency. For the mechanical cleaning, removal of fouling layers was facilitated using suction flow from an FDG, and the cleanliness of the membrane was characterised using *ImageJ* analysis. For all RCA membranes tested, FDG achieved 80% to 95% removal at shear stress values of 3.9 Pa, corresponding to a water velocity of 1.3 m s^{-1}. In contrast to chemical cleaning, FDG did not change the surface property of membrane after application. Chemical cleaning using *P3-Ultrasil 11* altered both the membrane surface hydrophobicity and the roughness. These results show that the fouling layer on RCA membranes can be removed by applying the FDG technique, without affecting the membrane surface modification previously caused by chemical cleaning.

Nomenclature

Abbreviations

CFV   cross-flow velocity (m s^{-1})

FDG   fluid dynamic gauging

LB   Liebermann-Buchard

MWCO molecular weight cut-off

PME   pectin methylesterase

PWF   pure water flux

R   rejection ratio

RCA   regenerated cellulose acetate

RO   reverse osmosis

TPC   total phytosterol content

UF   ultrafiltration

Symbols

A_u	absorbance of the sample
C_f	friction factor
C_p	solute concentration in the permeate (mg ml^{-1})
C_r	solute concentration in the retentate (mg ml^{-1})
C_s	concentration of stigmasterol in standard solution (mg ml^{-1})
d	tube inner diameter (m)
d_t	nozzle inner diameter (m)
h	distance between the gauge and fouling layer (m)
h_0	distance between the gauge and membrane (m)
J	flux through the membrane (L m^{-2} h^{-1})
m	gauging mass flow rate (kg s^{-1})
r	inner radius of the FDG nozzle (m)
R_{tot}	total resistance (m^{-1})
TMP	transmembrane pressure (Pa)
w	nozzle thickness (m)

Greek symbols

α	separation factor
ρ	fluid density (kg m^{-3})
τ	fluid shear stress (Pa)
τ_{wall}	wall shear stress (Pa)
μ	dynamic viscosity of fluid (Pa s)
μ_m	mean pipe flow velocity (m s^{-1})

Acknowledgements

Conflict of Interest

The authors declare that they have no conflicts of interest.

References

1. Gulec HA, Bagci PO, Bagci U. Clarification of Apple Juice Using Polymeric Ultrafiltration Membranes: a Comparative Evaluation of Membrane Fouling and Juice Quality. Food and Bioprocess Technology. 2017;10(5):875-85.

2. Cassano A, Conidi C, Ruby-Figueroa R, Castro-Muñoz R. Nanofiltration and Tight Ultrafiltration Membranes for the Recovery of Polyphenols from Agro-Food By-Products. Int J Mol Sci. 2018;19:351.

3. Lafi R, Gzara L, Lajimi RH, Hafiane A. Treatment of textile wastewater by a hybrid ultrafiltration/electrodialysis process. Chemical Engineering and Processing - Process Intensification. 2018;132:105-13.

4. Guo W, Ngo H-H, Li J. A mini-review on membrane fouling. Bioresource Technology. 2012;122:27-34.

5. Meng S, Zhang M, Yao M, Qiu Z, Hong Y, Lan W, et al. Membrane Fouling and Performance of Flat Ceramic Membranes in the Application of Drinking Water Purification. Water 2019;11:2606.

6. Argyle IS, Pihlajamäki A, Bird MR. Black tea liquor ultrafiltration: Effect of ethanol pre-treatment upon fouling and cleaning characteristics. Food and Bioproducts Processing. 2015;93(Supplement C):289-97.

7. Evans PJ, Bird MR, Rogers D, Wright CJ. Measurement of polyphenol–membrane interaction forces during the ultrafiltration of black tea liquor. Colloids and Surfaces A: Physicochemical and Engineering Aspects. 2009;335(1):148-53.

8. Mulder M. Basic Principles of Membrane Technology. Second ed. The Netherlands: Kluwer Academic Publishers; 1996.

9. Cassano A, Marchio M, Drioli E. Clarification of blood orange juice by ultrafiltration: analyses of operating parameters, membrane fouling and juice quality. Desalination. 2007;212(1):15-27.

10. Pap N, Mahosenaho M, Pongrácz E, Mikkonen H, Jaakkola M, Virtanen V, et al. Effect of Ultrafiltration on Anthocyanin and Flavonol Content of Black Currant Juice (Ribes nigrum L.). Food and Bioprocess Technology. 2012;5(3):921-8.

11. Echavarría AP, Torras C, Pagán J, Ibarz A. Fruit Juice Processing and Membrane Technology Application. Food Engineering Reviews. 2011;3(3):136-58.

12. Shi X, Tal G, Hankins NP, Gitis V. Fouling and cleaning of ultrafiltration membranes: A review. Journal of Water Process Engineering. 2014;1:121-38.

13. Park K-B, Choi C, Yu H-W, Chae S-R, Kim IS. Optimization of chemical cleaning for reverse osmosis membranes with organic fouling using statistical design tools. Environmental Engineering Research. 2018;23(4):474-84.

14. Aslam M, Charfi A, Lesage G, Heran M, Kim J. Membrane bioreactors for wastewater treatment: A review of mechanical cleaning by scouring agents to control membrane fouling. Chemical Engineering Journal. 2017;307:897-913.

15. Tuladhar TR, Paterson WR, Macleod N, Wilson DI. Development of a novel non-contact proximity gauge for thickness measurement of soft deposits and its application in fouling studies. The Canadian Journal of Chemical Engineering. 2000;78(5):935-47.

16. Chew YMJ, Paterson WR, Wilson DI. Fluid dynamic gauging: A new tool to study deposition on porous surfaces. Journal of Membrane Science. 2007;296(1):29-41.

17. Jones SA, Chew YMJ, Bird MR, Wilson DI. The application of fluid dynamic gauging in the investigation of synthetic membrane fouling phenomena. Food and Bioproducts Processing. 2010;88(4):409-18.

18. Mattsson T, Lewis WJT, Chew YMJ, Bird MR. In situ investigation of soft cake fouling layers using fluid dynamic gauging. Food and Bioproducts Processing. 2015;93:205-10.

19. Lewis WJT, Chew YMJ, Bird MR. The application of fluid dynamic gauging in characterising cake deposition during the cross-flow microfiltration of a yeast suspension. Journal of Membrane Science. 2012;405-406:113-22.

20. Abd-Razak NH, Zairossani MN, Chew YMJ, Bird MR. Fouling Analysis and the Recovery of Phytosterols from Orange Juice Using Regenerated Cellulose Ultrafiltration Membranes. Food and Bioprocess Technology. 2020;13(11):2012-28.

21. Abd-Razak NH, Pihlajamäki A, Virtanen T, John Chew YM, Bird MR. The influence of membrane charge and porosity upon fouling and cleaning during the ultrafiltration of orange juice. Food and Bioproducts Processing. 2021;126:184-94.

22. Weis A, Bird MR, Nyström M, Wright C. The influence of morphology, hydrophobicity and charge upon the long-term performance of ultrafiltration membranes fouled with spent sulphite liquor. Desalination. 2005;175(1):73-85.

23. Abd-Razak NH, Chew YMJ, Bird MR. Membrane fouling during the fractionation of phytosterols isolated from orange juice. Food and Bioproducts Processing. 2019;113:10-21.

24. Chew JYM, Paterson WR, Wilson DI. Fluid dynamic gauging for measuring the strength of soft deposits. Journal of Food Engineering. 2004;65(2):175-87.

25. Peck OPW, John Chew YM, Bird MR, Bolhuis A. Application of Fluid Dynamic Gauging in the Characterization and Removal of Biofouling Deposits. Heat Transfer Engineering. 2015;36(7-8):685-94.

26. Jiraratananon R, Chanachai A. A study of fouling in the ultrafiltration of passion fruit juice. Journal of Membrane Science. 1996;111(1):39-48.

27. Mbaebie BO, Edeoga HO, Afolayan AJ. Phytochemical analysis and antioxidants activities of aqueous stem bark extract of Schotia latifolia Jacq. Asian Pacific Journal of Tropical Biomedicine. 2012;2(2):118-24.

28. Sathishkumar T, Baskar R. Screening and quantification of phytochemicals in the leaves and flowers in the leaves and flowers of Tabernaemontana heyneana Wall. Indian Journal of Natural Products and Resources. 2014;5(3):237-43.

29. Cassano A, Donato L, Conidi C, Drioli E. Recovery of bioactive compounds in kiwifruit juice by ultrafiltration. Innovative Food Science & Emerging Technologies. 2008;9(4):556-62.

30. Kruger NJ. The Bradford method for protein quantitation. Methods in molecular biology (Clifton, NJ). 1994;32:9-15.

31. Zayas JF. Solubility of Proteins. Functionality of Proteins in Food. Berlin, Heidelberg: Springer Berlin Heidelberg; 1997. p. 6-75.

32. Aghajanzadeh S, Kashaninejad M, Ziaiifar AM. Cloud stability of sour orange juice as affected by pectin methylesterase during come up time: Approached through fractal dimension. International Journal of Food Properties. 2017;20(sup3):S2508-S19.

33. Goosen MFA, Sablani SS, Al-Maskari SS, Al-Belushi RH, Wilf M. Effect of feed temperature on permeate flux and mass transfer coefficient in spiral-wound reverse osmosis systems. Desalination. 2002;144(1):367-72.

34. Amy GL. NOM Rejection By, and Fouling Of, NF and UF Membranes: American Water Works Association; 2001.

35. Nguyen LAT, Schwarze M, Schomäcker R. Adsorption of non-ionic surfactant from aqueous solution onto various ultrafiltration membranes. Journal of Membrane Science. 2015;493(Supplement C):120-33.

36. Mohammad A, Hilal N, Ying Pei L, Nurul Hasyimah Mohd Amin I, Raslan R. Atomic Force Microscopy as a Tool for Asymmetric Polymeric Membrane Characterization. Sains Malaysiana. 2011;40(3):237-44.

37. Weis A, Bird MR, Nyström M. The chemical cleaning of polymeric UF membranes fouled with spent sulphite liquor over multiple operational cycles. Journal of Membrane Science. 2003;216(1):67-79.

Table 1: Mass balance and separation factor for total phytosterols and protein from orange juice by UF process with 10 kDa RCA membranes at; (a) 10 °C, (b) 20 °C and (c) 40 °C.

(a) At 10 °C	Feed	Permeate (% of feed)	Retentate (% of feed)	Total (%) (% of phytosterols or proteins in the retentate and permeate)
Volume (ml)	3000	600 (20%)	2400 (80%)	100
Total phytosterols (mg)	913	78 (9%)	707 (78%)	87
Protein (mg)	2911	25 (1%)	2235 (77%)	78
Concentration ratio (phytosterols to protein)	0.3	3.1		
Separation factor	10.3			

(b) At 20 °C	Feed	Permeate (% of feed)	Retentate (% of feed)	Total (%) (% of phytosterols or proteins in the

				retentate and permeate)
Volume (ml)	3000	850 (28%)	2150 (72%)	100
Total phytosterols (mg)	810	135 (17%)	504 (62%)	79
Protein (mg)	2910	26 (1%)	2408 (83%)	84
Concentration ratio (phytosterols to protein)	0.3	5.2		
Separation factor	17.3			

(c) At 40 °C	Feed	Permeate (% of feed)	Retentate (% of feed)	Total (%) (% of phytosterols or proteins in the retentate and permeate)
Volume (ml)	3000	1200 (40%)	1800 (60%)	100
Total phytosterols (mg)	755	190 (25%)	441 (58%)	83
Protein (mg)	2807	317 (13%)	1721 (61%)	74
Concentration ratio (phytosterols to protein)	0.3	0.6		
Separation factor	2.0			

Table 2: Mass balance and separation factor for total phytosterols and protein separated from orange juice by UF process using 10 kDa RCA membranes at different feed volume; (a) 3 L, (b) 6 L and (c) 9L.

(a) 3 L	Feed	Permeate (% of feed)	Retentate (% of feed)	Total (%)
Volume (ml)	3000	850 (28%)	2150 (72%)	100
Total phytosterols (mg)	810	135 (17%)	504 (62%)	79
Protein (mg)	2910	26 (1%)	2408 (83%)	84
Concentration ratio (phytosterols to protein)	0.3	5.2		
Separation factor	17.3			

(b) 6 L	Feed	Permeate (% of feed)	Retentate (% of feed)	Total (%)
Volume (ml)	6000	800 (13%)	5200 (87%)	100
Total phytosterols (mg)	1620	137 (9%)	1155 (71%)	80
Protein (mg)	5760	35 (1%)	4420 (77%)	78
Concentration ratio (phytosterols to protein)	0.3	3.9		
Separation factor	13.0			

(c) 9 L	Feed	Permeate (% of feed)	Retentate (% of feed)	Total (%)
Volume (ml)	9000	800 (9%)	8200 (91%)	100
Total phytosterols (mg)	2430	147 (6%)	1885 (78%)	84
Protein (mg)	8640	32 (1%)	6560 (76%)	77
Concentration ratio (phytosterols to protein)	0.3	4.6		
Separation factor	15.3			

Table 3 Results of contact angles measurement.

Membrane	Hydrophobicity (° contact angle)					
	Conditioned	F1	F1→CC	F1→FDG	F1→CC →F2	F1→CC →F2→FDG
RCA 10 kDa	11 ± 2	10 ± 2	8 ± 2	11 ± 2	10 ± 2	8 ± 2
RCA 30 kDa	13 ± 2	10 ± 2	12 ± 2	13 ± 2	10 ± 3	11 ± 2
RCA 100 kDa	18 ± 2	10 ± 2	15 ± 2	17 ± 2	11 ± 3	14 ± 2

Table 4 Surface roughness values from AFM analysis.

Membrane	Surface Roughness (nm)					
	Conditioned	F1	F1→CC	F1→FDG	F1→CC →F2	F1→CC →F2→FDG
RCA 10 kDa	3 ± 1	31 ± 2	10 ± 2	8 ± 2	33 ± 2	12 ± 2
RCA 30 kDa	17 ± 1	42 ± 3	20 ± 2	18 ± 2	40 ± 2	21 ± 2
RCA 100 kDa	10 ± 2	39 ± 2	15 ± 1	11 ± 2	38 ± 2	15 ± 3
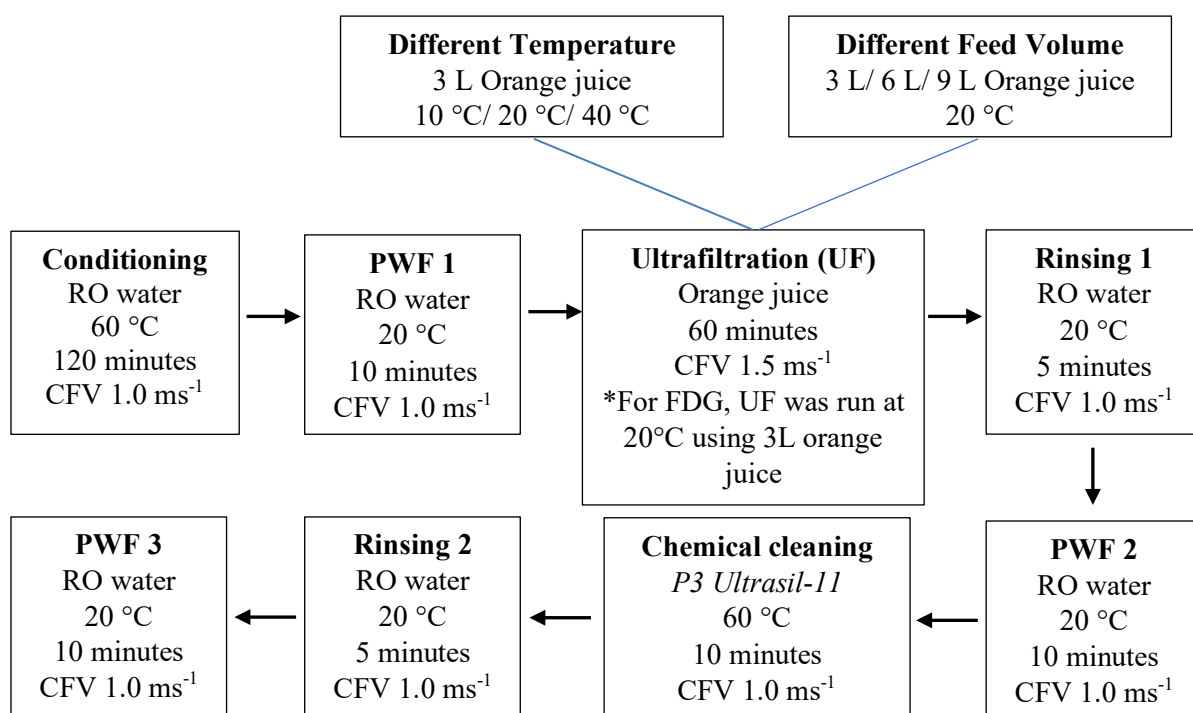
Figure 1: Summary of ultrafiltration experiments. All steps were run at TMP 1.0 bar. The 10 kDa membrane was used to study the effect of feed conditions. The UF step was run at 20 °C using 10 kDa, 30 kDa and 100 kDa RCA membranes to study the effect of membrane cleaning.
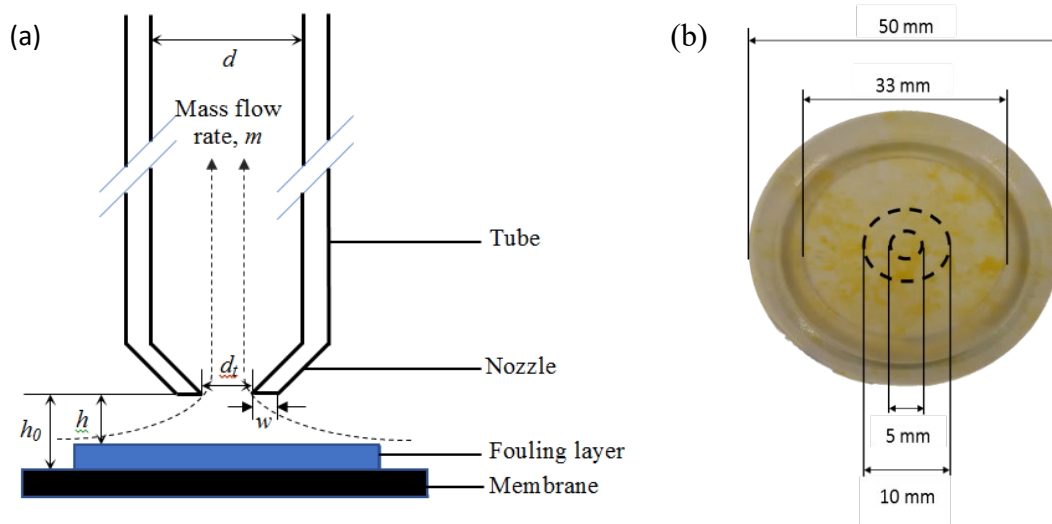
Figure 2: (a) Schematic of a FDG nozzle showing dimensions, where the nozzle inner diameter, d_t = 5 mm, tube inner diameter, d = 25 mm and nozzle thickness, w = 2 mm; (b) example of a membrane fouled by orange juice, where dashed line shows a dimension of the nozzle inner diameter, d_t = 5 mm and nozzle outer diameter = 10 mm.
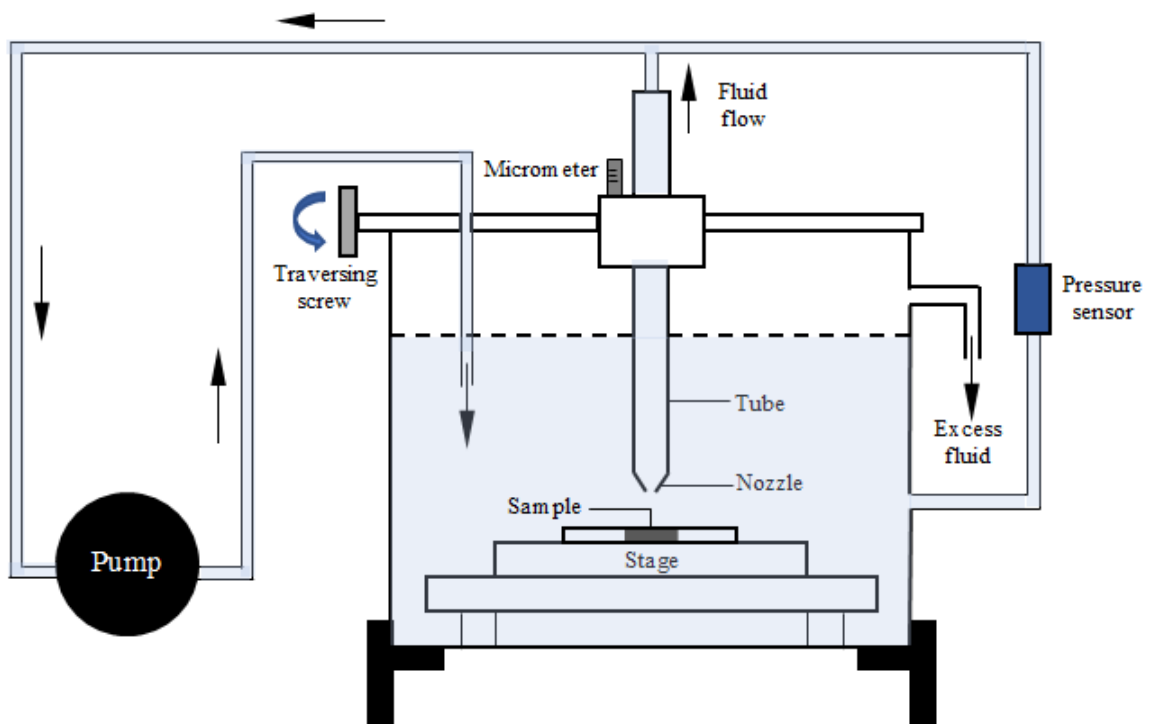
Figure 3: Schematic of the FDG test rig used in this study. The fluid used was RO water.
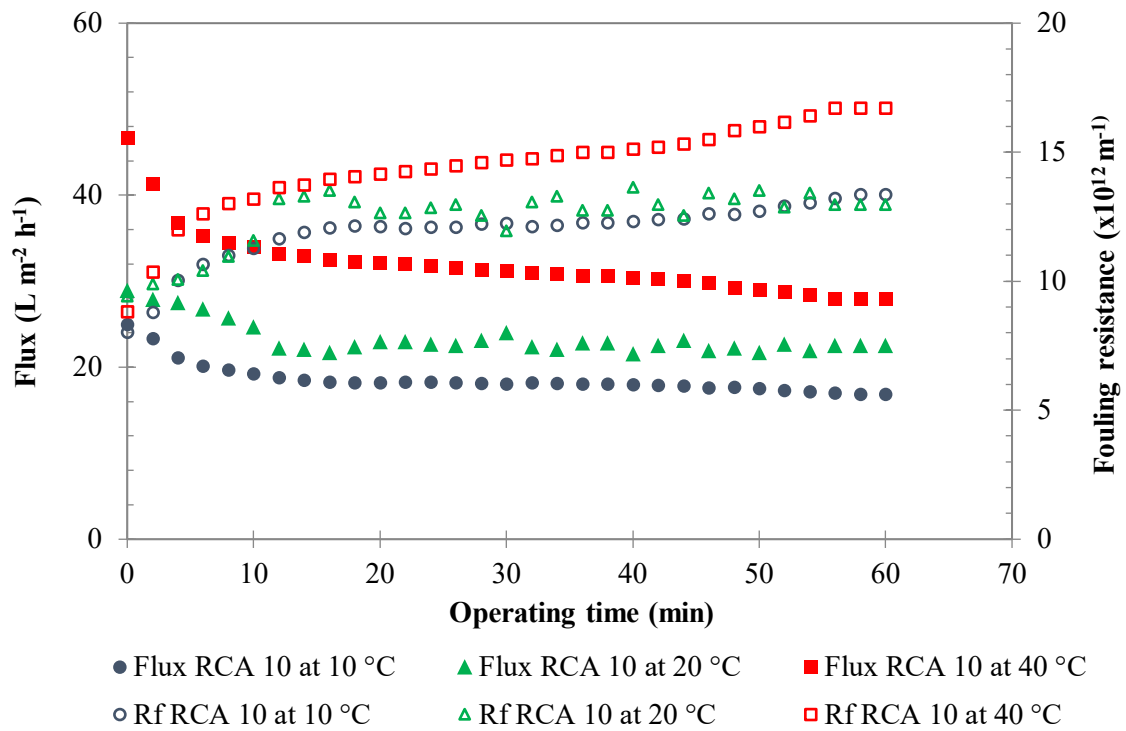
Figure 4: Permeate flux and total fouling resistance for RCA membranes tested at different temperatures. The largest error for this set of data is ± 1.5 L m^{-2} h^{-1}. Closed symbols in Figure 6 represent the permeate fluxes, and open symbols represent the total fouling resistances.
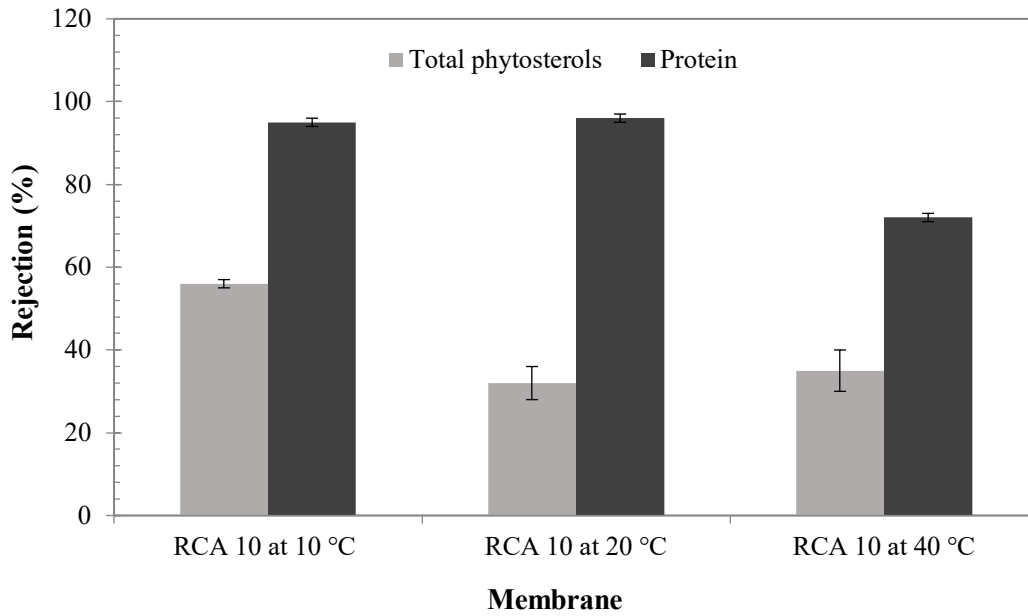
Figure 5: Rejection of total phytosterols and proteins by RCA 10 kDa membranes at different temperatures.
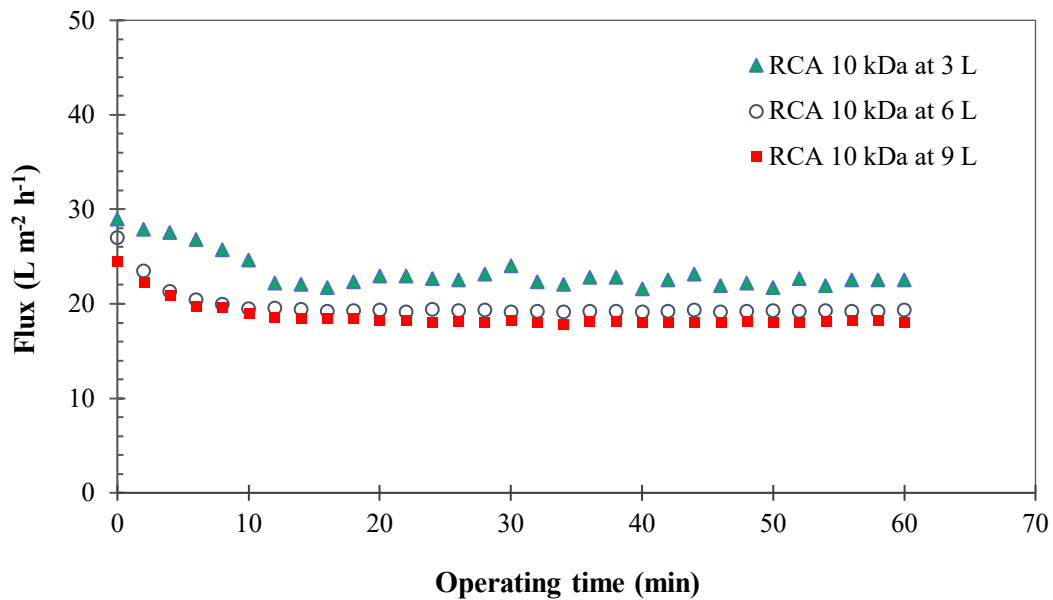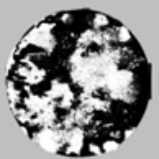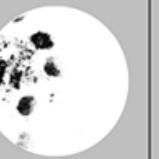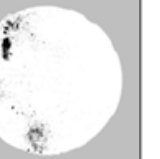
Figure 6: Permeate flux decline for RCA membranes tested at different feed volume at 20 °C. The largest error for this set of data is ± 1.5 L m⁻² h⁻¹.

(a) RCA 10 kDa (**(F1) → (FDG)**)

h/dt	No gauging	0.15	0.10	0.06	0.04
Shear stress [Pa]	0	0.28	0.62	1.73	3.90
Image J					
% Surface coverage (ImageJ)	84 ± 2	57 ± 2	35 ± 3	11 ± 3	4 ± 2
Area/ Area$_0$	1.00	0.68 ± 0.02	0.42 ± 0.03	0.13 ± 0.03	0.05 ± 0.01

(b) RCA 30 kDa (**(F1) → (CC) → (F2) → (FDG)**)

h/dt	No gauging	0.15	0.10	0.06	0.04
Shear stress [Pa]	0	0.28	0.62	1.73	3.90
Image J					
% Surface coverage (ImageJ)	94 ± 2	74 ± 3	62 ± 2	36 ± 2	13 ± 2
Area/ Area$_0$	1.00	0.79 ± 0.02	0.66 ± 0.01	0.39 ± 0.01	0.14 ± 0.02

Figure 7: Surface coverage of the RCA membranes after FDG cleaning analysed by *ImageJ*; (a) RCA 10 kDa (**(F1) → (FDG)**), and (b) RCA 30 kDa (**(F1) → (CC) → (F2) → (FDG)**).
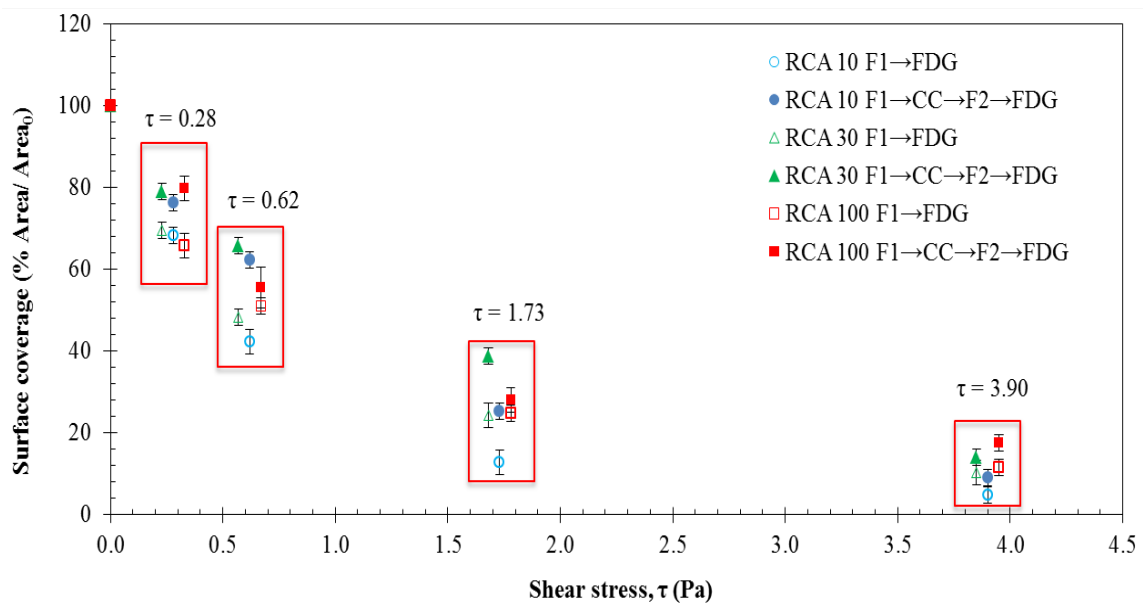

Figure 8: Surface coverage of RCA membranes after FDG cleaning at four different shear stress values.

22

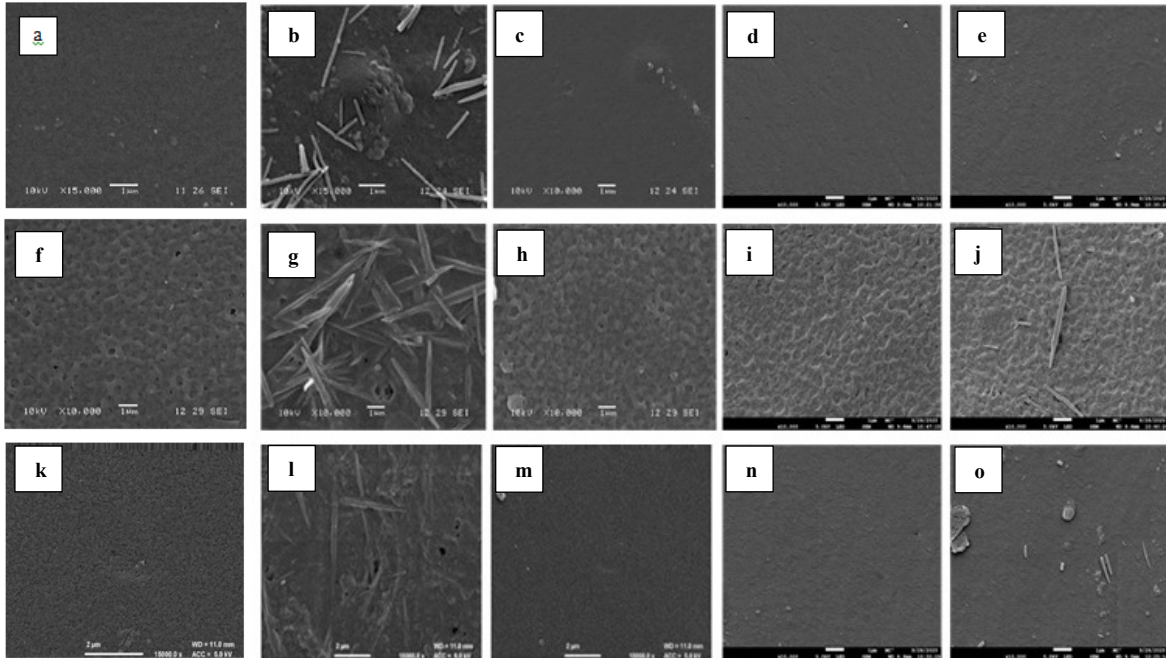| | (1)
Conditioned | (2)
Fouled 1 (F1) | (3)
Fouled 1
(F1) →
Chemical
cleaning (CC) | (4)
Fouled 1
(F1) → Fluid
dynamic
gauging (FDG) | (5)
Fouled 1
(F1) →(CC) →
Fouled 2
(F2) → (FDG) |

Figure 9: Scanning electron microscope (SEM) images of conditioned RCA membranes, after fouling and cleaning; (a) to (e) RCA 10 kDa, (f) to (j) RCA 30 kDa and (k) to (o) RCA 100 kDa membranes.